Highly Diastereoselective Functionalization of Piperidines by Photoredox Catalyzed α-Amino C–H Arylation and Epimerization

Morgan M. Walker[†], **Brian Koronkiewicz**[†], **Shuming Chen**[‡], **K. N. Houk**[*,‡], **James M. Mayer**[*,†], **Jonathan A. Ellman**[*,†]

[†] Department of Chemistry, Yale University, New Haven, Connecticut 06520, United States

[‡] Department of Chemistry and Biochemistry, University of California, Los Angeles, California 90095, United States

Abstract

We report a photoredox catalyzed α-amino C–H arylation reaction of highly substituted piperidine derivatives with electron deficient cyano(hetero)arenes. The scope and limitations of the reaction were explored, with piperidines bearing multiple substitution patterns providing the arylated products in good yields and with high diastereoselectivity. In order to probe the mechanism of the overall transformation, optical and fluorescent spectroscopic methods were used to investigate the reaction. By employing flash-quench transient absorption spectroscopy, we were able to observe electron transfer processes associated with radical formation beyond the initial excited state Ir(ppy)$_3$ oxidation. Following the rapid and unselective C–H arylation reaction, a slower epimerization occurs to provide the high diastereomer ratio observed for a majority of the products. Several stereoisomerically pure products were re-subjected to the reaction conditions, each of which converged to the experimentally observed diastereomer ratios. The observed distribution of diastereomers corresponds to a thermodynamic ratio of isomers based upon their calculated relative energies using density functional theory (DFT).

Graphical Abstract

*Corresponding Author: jonathan.ellman@yale.edu, james.mayer@yale.edu, houk@chem.ucla.edu.

The authors declare no competing financial interest.

ASSOCIATED CONTENT
The Supporting Information is available free of charge on the ACS Publications website at DOI:
Experimental procedures, characterization data, crystallographic data, optical and fluorescence quenching studies, and Cartesian coordinates of all computed structures.

INTRODUCTION

Piperidines are by far the most prevalent of all heterocycles found in drugs.[1] For example, the piperidine substructure is present in the blockbuster antidepressant paroxetine, morphine along with its congeners, many of the anti-histamine class of drugs, and tofacitinib used in the treatment of arthritis and ulcerative colitis.[1] Substitution about the piperidine scaffold is extremely common,[1a] and for this reason, efficient new methods for the diastereoselective elaboration of the piperidine framework have the potential to greatly facilitate the discovery of new pharmaceutical agents.

Photoredox catalysis utilizing transition metalpolypyridyl complexes has provided a powerful strategy to access novel reactivity manifolds.[2] Although the utility of α-amino radicals has long been appreciated,[3] the MacMillan group provided a seminal study using a transition metal photoredox catalyst for the synthesis of α-branched amines via α-amino radical coupling with electron deficient cyano(hetero)arene derivatives (Scheme 1A).[4,5] Following this report, many groups have developed transformations using α-amino radicals as the reactive intermediate for additions to alkenes and other unsaturated π-bonds,[6] cross-coupling with (hetero)arenes,[7] and other coupling partners.[8]

Achieving stereoselective transformations is one of the major challenges for photoredox catalysis because radicals serve as key reactive intermediates.[9] In this regard, significant advances have been realized for the asymmetric synthesis of α-branched amines via α-amino radical intermediates using photoredox catalysts often in combination with other modes of catalysis.[10] Approaches for the diastereoselective synthesis of α-branched amines to produce compounds that incorporate two or more stereogenic centers via α-amino radical intermediates have also been developed.[10c,11] However, the elaboration of complex molecules incorporating stereogenic center(s) requires that diastereoselectivity be achieved relative to the pre-existing stereogenic center(s). This type of stereoselective transformation has rarely been explored for photoredox catalyzed α-amino radical reactions.[11b,12,13]

Although the reactivity of α-amino radicals can introduce challenges for achieving stereoselective transformations, the low inversion barrier for these radicals also provides new opportunities for stereoselective synthesis by epimerization. Pioneering studies by Bertrand and coworkers demonstrated that a thiyl radical could mediate the racemization of benzylic amines through reversible hydrogen abstraction.[14] Very recently, Knowles and Miller have achieved an impressive photo-driven deracemization of cyclic ureas based on the use of excited-state redox events.[10a] Moreover, in a photoredox catalyzed reverse polarity Povarov annulation to give disubstituted tetrahydroquinolines, an increase in diastereoselectivity to 18:1 was observed when the initial 10:1 ratio of product diastereomers was re-submitted to the reaction conditions.[11e,15,16]

Herein, we report the development of a highly diastereoselective Ir(III) photoredox catalyzed reaction cascade that proceeds by α-amino C–H arylation of densely functionalized piperidines **1** followed by epimerization at the α-position to give the most stable stereoisomer **2** (Scheme 1B). Notably, differentially substituted piperidine derivatives with up to four stereogenic centers were effective substrates, providing the products with

generally high diastereoselectivity relative to the pre-existing stereogenic centers. We propose mechanisms for both the C–H arylation reaction and epimerization steps based on an array of spectroscopic studies and time courses for product formation. Our results are consistent with an unselective photoredox C–H arylation followed by product epimerization leading to the observed diastereoselectivity. The diastereomers underwent oxidation with comparable rate constants, and therefore, product oxidation kinetics were not responsible for the epimerization diastereoselectivity. We subjected the separate diastereomers to the photoredox-catalyzed reaction conditions, and each yielded the experimentally observed distribution of diastereomers suggesting that the reaction is under thermodynamic control. The calculated relative energies of the diastereomers using density functional theory (DFT) correlate with the observed diastereomer ratios.

RESULTS AND DISCUSSION

Efficient Preparation of Piperidine Starting Materials

1. We first developed a facile two-step route to diastereomerically pure, densely substituted piperidines **1** from readily available precursors (Scheme 2). Previously, we reported a Rh(I)-catalyzed C–H activation/electrocyclization cascade to furnish highly substituted 1,2-dihydropyridines **4** from imines **3** and internal alkynes.[17] Catalytic hydrogenation of dihydropyridines **4** with Pd/C then provides piperidines **1** (see Supporting Information for optimization Table S1 and experimental details).[18] In all cases, only the all-cis stereoisomer was detected and was isolated in 63% average overall yield for the two step process.

Optimization and Scope of C–H Arylation

To optimize the yield and diastereoselectivity of the C–H arylation reaction, we explored a variety of conditions for arylating trisubstituted piperidine **1a** (R^1 = H, R^2 = Me, R^3 = R^4 = Et) with 1,4-dicyanobenzene (DCB) to give **2a** (Tables S2 and S3 in the Supporting Information). Ir(ppy)$_3$ (ppy = 2-phenylpyridine) was determined to be the optimal photocatalyst for the α-arylation, in agreement with MacMillan's earlier report.[4,19] Of particular note, we were able to employ the piperidine as the limiting reagent to give **2a** in high yield and with high diastereoselectivity (Table 1). For this transformation, arylation unambiguously provided the syn isomer as determined by X-ray crystallography.

The optimized conditions were next applied to a number of piperidine derivatives using DCB as the coupling partner (Table 1). Piperidines with the strained cyclopropyl ring (**2b**) and the linear propyl chain (**2c**) at R^2 were effective substrates in the reaction. A phenyl substituent could also be incorporated at the R^2 position to provide product **2d** in good yield and with high diastereoselectivity, although a longer reaction time of 16 h was required.

Trisubstituted piperidines with a different substitution pattern also provided the arylated products in high yield and diastereoselectivity as exemplified for **2e-2k**. However, for this substitution pattern, the anti-stereoisomer was obtained, as unambiguously determined by X-ray crystallography for **2e**. Piperidines with cyclopentyl (**2f**), Boc protected piperidine (**2g**), and isopropyl (**2h**) at R^4 were all effective substrates in the reaction. Notably, arylation of the *N*-Boc piperidine in **2g** does not occur under our reaction conditions, due to the

thermodynamically unfavorable oxidation of electron-deficient carbamates.[20] Different *N*-aryl substituents were also evaluated, with products **2h-2k** each obtained in good to high yields and with excellent diastereoselectivities. However, for alkyl, acyl and toluenesulfonyl substituents on the piperidine nitrogen, no coupling was observed (for a full list of unsuccessful reactants, see Table S4 in the Supporting Information).

Arylation of a tetrasubstituted piperidine gave the fully substituted piperidine product **2l** in high yield and with 85:15 diastereoselectivity for the anti isomer.[21] A monosubstituted piperidine also arylated in high yield to give product **2m** with modest diastereoselectivity and with a preference for the syn isomer.[21]

Using piperidine **1a**, we explored the scope with respect to the cyano(hetero)arene coupling partner (**2n-2q**). Heterocycles, such as for 4-cyanopyridine, provided product **2n** in moderate yield and with high selectivity. The desired products were also obtained in moderate to good yields for other electron deficient cyanoarenes, including a para substituted morpholine amide (**2o**), phthalide (**2p**) and ethyl ester (**2q**). Arylation with the electron-rich 4-methoxybenzonitrile and the electron-neutral cyanobenzene were not successful, consistent with the redox potentials of these derivatives[22] and with MacMillan's initial report on tertiary aniline arylation.[23,4] MacMillan has successfully coupled heteroaryl chlorides with unhindered tertiary anilines;[24] however, with our more hindered, substituted piperidines less than 10% coupling occurred with 2-chlorobenzothiazole (for a full list of unsuccessful reactants, see Table S4 in the Supporting Information). All of the cyano(hetereo)arene coupling partners were additionally explored with a trisubstituted piperidine with a different substitution pattern and provided products **2r**-**2u** in moderate to good yields and with excellent diastereoselectivities in all cases.

The large majority of piperidines that we investigated for arylation were efficiently prepared by face selective hydrogenation of DHPs **4** to give the all-syn substituted diastereomer **1** (see Scheme 2). To demonstrate the potential generality of the approach to other stereoisomers, we also evaluated the arylation of diastereomer **5** (eq 1), which displayed the 3-ethyl group anti to the two other alkyl substituents (for the synthesis of **5,** see the Supporting Information). Under the standard reaction conditions, product **2v** was obtained in good yield and with 84:16 diastereoselectivity.

We further explored functional group compatibility of the reaction by evaluating readily accessible 4-substituted piperidines (Table 2). These unhindered piperidine substrates are capable of over-addition, which introduces an added challenge for obtaining high product yields. For photoredox mediated arylations of unhindered tertiary anilines, over-addition is typically minimized by using excess of the tertiary amine substrate.[4] We instead chose to employ the DCB coupling partner in a 1:1 stoichiometry because the substituted piperidines are the more expensive of the two inputs. Even with this stoichiometry, the acetamide substituted piperidine provided the arylated product **2w** in excellent yield though with modest diastereoselectivity. Products were also obtained in reasonable yields and modest diastereoselectivities for hydroxy (**2x**), hydroxymethyl (**2y**), and methoxymethyl (**2z**) substituents at the 4-position.
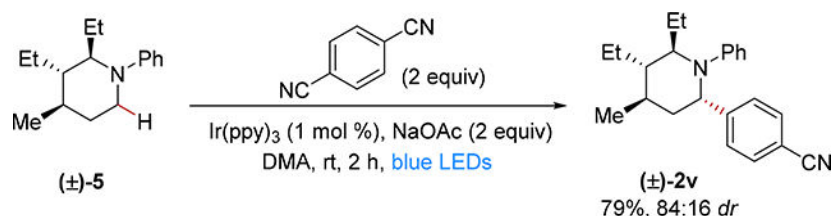
(1)

Mechanistic Investigations

To better understand the mechanism of product formation, we investigated the reactivity of the Ir(ppy)$_3$ photosensitizer and DCB intermediates using optical and fluorescent spectroscopies. Upon irradiation at 450 nm, the Ir complex undergoes a metal-to-ligand charge transfer followed by rapid intersystem crossing to give the long-lived triplet state that engages in single electron transfer.[25] Based on the reduction potential of *Ir(ppy)$_3$ (*$E_{1/2}$(Ir$^{IV/*III}$) = −1.73 V *vs.* SCE in MeCN)[26] and DCB (DCB/DCB$^{\cdot-}$ E_p = −1.61 V *vs.* SCE in MeCN),[27] we would expect an oxidative quenching mechanism to be operative, generating Ir^{IV} and the DCB$^{\cdot-}$ in the first step as depicted in Figure 1A. Indeed, luminescence quenching studies revealed fast electron transfer (ET) between DCB and *Ir(ppy)$_3$, occurring with a rate constant k$_{quench}$ = 2.9 × 10^9 M^{-1}s^{-1} in *N,N*-dimethylacetamide (DMA). In contrast, high concentrations of piperidine **1m** caused minimal change in the *Ir(ppy)$_3$ lifetime (see Figure S2 in the Supporting Information). These data, and the experimental excess of DCB, support an initial excited state ET producing Ir(ppy)$_3^+$ and DCB$^{\cdot-}$ and are also in agreement with MacMillan's previous observations.[4]

In order to examine the reactivity of these photoproducts, we pursued the visible absorption spectra for each. We obtained authentic absorption spectra for Ir(ppy)$_3^+$ from spectroelectrochemical oxidation of Ir(ppy)$_3$ in DMA (see Figure S3 in the Supporting Information), and found authentic spectra for the DCB$^{\cdot-}$ in the pulse radiolysis literature.[28] We fortuitously observed an isosbestic point for the Ir(ppy)$_3$ to Ir(ppy)$_3^+$ conversion at 346 nm, very close the λ$_{max}$ of the DCB$^{\cdot-}$ species. This allowed us to observe absorption changes at 346 nm that correspond only to the evolution of DCB$^{\cdot-}$.

The reactivity of the Ir(ppy)$_3^+$ and DCB$^{\cdot-}$ species is not visible in luminescence quenching studies, and so we turned to flash-quench transient absorption spectroscopy (TA) to observe the ground state reactivity of these photogenerated species. In the absence of piperidine substrate, Ir(ppy)$_3^+$ and DCB$^{\cdot-}$ recombine at or near the diffusion limit (Figure 1C), which we can follow at 346 nm for the DCB$^{\cdot-}$ decay and at 390 nm for the Ir(ppy)$_3^+$ decay (Figure 1B, S4 and S5 in the Supporting Information). This recombination follows an equal concentration bimolecular kinetic model (see Supporting Information). With added piperidine **1m**, Ir(ppy)$_3^+$ is reduced back to Ir(ppy)$_3$ more rapidly, consistent with piperidine oxidation by Ir(ppy)$_3^+$ to form the aminium radical cation **7m** and Ir(ppy)$_3$ (Figure 1A, S5 in the Supporting Information). In agreement with this observation, increasing concentration of piperidine **1m** leads to larger residual absorbance for the DCB$^{\cdot-}$ at 346 nm because the

$Ir(ppy)_3^+$ that is consumed by piperidine oxidation is unable to recombine with $DCB^{•−}$ (Figure 1C, S5 in the Supporting Information). Piperidine oxidation by $Ir(ppy)_3^+$ is consistent with the reduction potentials of the two species, $(E_{1/2}(Ir^{IV/III}) = 0.77$ V *vs.* SCE in MeCN) for the $Ir(ppy)_3$ catalyst,[26] versus the aminium cation ($E_p = +0.71$ V *vs.* SCE in MeCN for *N,N*-dimethylaniline).[29] From the piperidine concentration dependent reformation of $Ir(ppy)_3$ observed at 390 nm, we estimate a rate constant for piperidine oxidation $k_{ox,1m} = 2.4 \times 10^7$ $M^{−1}s^{−1}$ in DMA (see Figure S6 in the Supporting Information).

Under the conditions of our luminescence quenching and TA measurements, the photoinduced formation of $DCB^{•−}$ and the piperidine radical cation seems plausible. We did not observe further radical coupling reactions involving the persistent $DCB^{•−}$ by TA or by transient absorption IR experiments, specifically searching for new CN containing photoproducts. We therefore turned to quantum yield measurements to determine the plausibility of a closed-loop photoredox mechanism under the C–H arylation conditions. We used Scaiano's method[30] to determine the quantum yield of the reaction between **1a** and DCB. The quantum yield was calculated to be $\Phi = 0.5$ at early conversions, indicating that the photoredox catalyzed cycle is reasonable, although radical chain pathways cannot be ruled out.[31]

Taken together, these findings support the proposed mechanism shown in Figure 1D, which is consistent with MacMillan's original hypothesis.[4] Ir^{III} is excited by blue light to produce the excited state $*Ir^{III}$, which transfers an electron to DCB to generate the Ir^{IV} species and the DCB radical anion. ET from the piperidine **1m** to the Ir^{IV} regenerates Ir^{III}. The formed amine radical cation **7m** undergoes deprotonation at the α position by either NaOAc or the piperidine starting material or product, to deliver the α-amino radical **8m**, which can undergo a radical-radical coupling with the persistent DCB radical anion.[32] Following coupling to form **9m**, extrusion of cyanide furnishes the arylated piperidine **2m** and closes the catalytic cycle.

Epimerization studies

We sought to better understand the origins of the high diastereoselectivity observed under the reaction conditions, especially given that our postulated mechanism suggests that the C–C bond forming step is a radical-radical coupling.[9b] Surprisingly, when monitoring the progress of the reaction of piperidine **1a** and DCB over time, we observed that the initial reaction is not stereoselective (Figure 2). In fact, at 16 min, the ratio of the syn to anti isomer is 50:50 with 75% of the product already formed. Over the course of the remaining 2 h, the anti product isomer **2a-anti** epimerizes to the observed syn diastereomer **2a-syn**, which is ultimately obtained in >95:5 *dr*.[11e] Additionally, if the reaction is irradiated for 16 min followed by stirring in the dark for the remaining 2 h, the *dr* is 56:36 slightly favoring **2a-anti**, indicating that epimerization is a light driven process (see Table S5 in the Supporting Information).

In an effort to elucidate the mechanism of epimerization, we isolated the anti diastereomer **2a-anti** (>95:5 *dr*) and subjected it to the reaction conditions (Table 3). Notably, we obtained only the syn diastereomer **2a-syn** (>95:5 *dr*) in 85% yield after 2 h (Table 3, entry 1).

Epimerization was next evaluated upon removing different reaction components. Complete epimerization to the syn diastereomer **2a-syn** was still obtained when NaOAc was removed (Table 3, entry 2), indicating that NaOAc does not play a significant role in the epimerization mechanism. When DCB was removed, only 21% of the product epimerized, with the unreacted anti isomer **2a-anti** recovered in 67% yield (Table 3, entry 3). Similar results were obtained when both DCB and NaOAc were removed (Table 3, entry 4). These observations suggest that significant epimerization only occurs under conditions that were shown to produce $Ir(ppy)_3^+$ upon irradiation.

To further explore this hypothesis, we postulated that a more oxidizing photocatalyst could directly form the piperidine radical cation by excited state electron transfer, without the need for initial quenching by DCB. To this end, we employed $[Ir(dtbbpy)(ppy)_2]PF_6$ (dtbbpy = 4,4'-di-*tert*-butyl-2,2'-bipyridine, $*E_{1/2}(Ir^{III/II})$) = 0.66 V *vs.* SCE in MeCN), whose excited state reduction potential is significantly more positive than that of $Ir(ppy)_3$.[25,33] Indeed, subjecting the anti diastereomer **2a-anti** to $[Ir(dtbbpy)(ppy)_2]PF_6$ under blue light, and in the absence of DCB, delivers the major diastereomer **2a-syn** as the only detectable product in 72% yield (Table 3, Entry 5). These results are consistent with an epimerization mechanism that proceeds through initial product piperidine oxidation (Table 3).

Based on these collective results, we propose the following mechanism for epimerization under the optimized reaction conditions with $Ir(ppy)_3$ (see Table 3): Excited state quenching by DCB gives potent oxidant $Ir(ppy)_3^+$. ET from **2a-anti** and perhaps also **2a-syn** followed by deprotonation yields α-amino radical **8a**. This intermediate then equilibrates to the **2a-syn** isomer through subsequent reprotonation and ET.

We next investigated whether or not the diastereoselectivity was a result of kinetic control as has been observed for other photoredox-catalyzed isomerization reactions.[34,10a] Specifically, one possibility for kinetic control would require that the piperidine diastereomers undergo initial ET oxidation at different rates leading to steady-state concentrations of the diastereomers (Figure 3). To evaluate this hypothesis, we measured the rate constants for oxidation of stereoisomerically pure **2a-syn** and **2a-anti** by $Ir(ppy)_3^+$ using TA spectroscopy. To account for the observed >19:1 **2a-syn:2a-anti** ratio, kinetically controlled selectivity would require that the rate constant for **2a-anti** oxidation ($k_{ox,anti}$) is at least 19 times larger than the rate constant for **2a-syn** ($k_{ox,syn}$), which would lead to depletion of **2a-anti** and enrichment of **2a-syn** under our reaction conditions. However, we determined that $k_{ox,anti}$ and $k_{ox,syn}$ were the same within error, indicating that the relative rate constants for piperidine oxidation were not responsible for the observed high selectivity. We can conclude that the epimerization is not kinetically controlled by initial oxidation to the aminium radical cations **7a**.

We therefore investigated whether or not the epimerization reaction could be under thermodynamic control. The proton transfer between **7a-syn** and **7a-anti** could generate an equilibrium mixture of diastereomers which controls the observed distribution of **2a** diastereomers. Such an equilibrium should be achievable starting with either diastereomer. To probe this possibility, we examined piperidine **2m**, which gave a quantifiable mixture of diastereomers under the reaction conditions (Scheme 3). We subjected both **2m-syn** and **2m-**

anti separately to epimerization with the photocatalyst [Ir(dtbbpy)(ppy)$_2$]PF$_6$. After 90 min of irradiation of the syn diastereomer **2m-syn**, a 70:30 (syn:anti) mixture of stereoisomers was obtained in 91% yield. Furthermore, subjecting the anti diastereomer **2m-anti** to the same conditions, gave a 78:22 (syn:anti) mixture of isomers and 94% recovery. Taken together, these results suggest that the observed diastereoselectivity can be approached from either diastereomer, which is consistent with a thermodynamically controlled process. However, this result does not rule out that the observed selectivity is due to a kinetically controlled steady state.[10a]

Further evidence for a thermodynamically controlled epimerization was obtained using DFT calculations to determine the relative stability of various arylated piperidine diastereomers (Table 4). We reasoned that the relative stability of the **2-syn** and **2-anti** diastereomers and the **7-syn** and **7-anti** aminium radical cation diastereomers would be similarly affected by the piperidine substituents. The calculated relative free energies of **2-syn** and **2-anti** piperidine isomers correlate with the observed diastereomer ratios. For the less substituted piperidine **2m**, the **2m-syn** isomer was calculated to be 0.6 kcal/mol lower in energy than the **2m-anti** isomer, consistent with the modest 63:37 syn:anti diastereoselectivity (Table 4, Entry 1). For piperidine **2a**, the **2a-anti** isomer is calculated to be 1.3 kcal/mol higher in energy than the experimentally obtained **2a-syn** isomer (Table 4, Entry 2). This preference is likely due to the **2a-anti** isomer having two axial alkyl substituents in the lowest-energy conformation (ethyl at R^4 and methyl at R^2), while the **2a-syn** isomer only has one. For piperidine **2e**, the difference in energy is more pronounced, with the **2e-syn** isomer disfavored by 4.3 kcal/mol (Table 4, Entry 3). In this case, the aryl substituent and the ethyl group at R^4 are calculated to be axial in the lowest energy conformation of **2e-syn**. Typically, aryl substituents have much higher A values than secondary alkyl carbons,[35] likely causing the **2e-anti** isomer to be significantly more favored.

CONCLUSIONS

We have described the highly diastereoselective α-amino C–H arylation of densely substituted piperidine derivatives. This study represents a rare example of utilizing photoredox catalysis to promote diastereoselective transformations of complex molecules containing pre-existing stereogenic centers. Key to the generally high selectivity was an epimerization reaction that followed a rapid and non-selective C–H arylation. The observed selectivities for the overall transformation correlate to the calculated relative stabilities of the diastereomers. We anticipate that epimerization processes should be applicable to efficient, diastereoselective syntheses of many different classes of nitrogen heterocycles. Towards this end, efforts are underway in our laboratories.

Supplementary Material

Refer to Web version on PubMed Central for supplementary material.
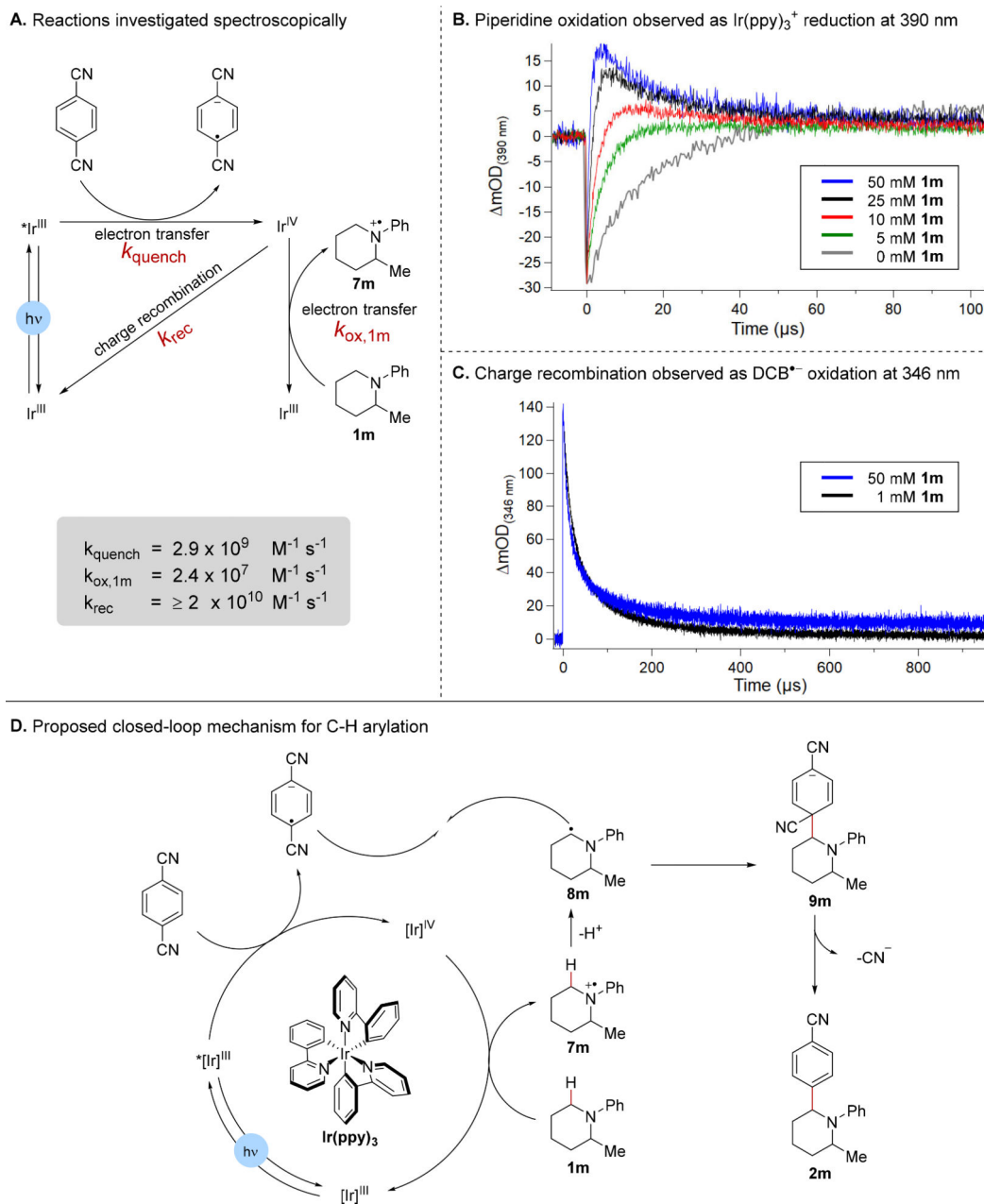
ACKNOWLEDGMENT

REFERENCES

1 (a). Vitaku E; Smith DT; Njardarson JT Analysis of the Structural Diversity, Substitution Patterns, and Frequency of Nitrogen Heterocycles among U.S. FDA Approved Pharmaceuticals. J. Med. Chem. 2014, 57, 10257. [PubMed: 25255204] (b)Typing the name of these drug and drug candidates into PubChem (http://pubchem.ncbi.nlm.nih.gov/) provides the compound structure, bioactivity, full list of published studies, and information regarding ongoing clinical trials, applications, and usage.

2 (a). Schultz DM; Yoon TP Solar Synthesis: Prospects in Visible Light Photocatalysis. Science 2014, 343, 1239176. [PubMed: 24578578] (b)Prier CK; Rankic DA; MacMillan DWC Visible Light Photoredox Catalysis with Transition Metal Complexes: Applications in Organic Synthesis. Chem. Rev. 2013, 113, 5322. [PubMed: 23509883] (c)Narayanam JMR; Stephenson CRJ Visible light photoredox catalysis: applications in organic synthesis. Chem. Soc. Rev. 2011, 40, 102. [PubMed: 20532341]

3 (a). Cho DW; Yoon UC; Mariano PS Studies Leading to the Development of a Single-Electron Transfer (SET) Photochemical Strategy for Syntheses of Macrocyclic Polyethers, Polythioethers, and Polyamides. Acc. Chem. Res. 2011, 44, 204. [PubMed: 21197953] (b)Pandey G; Reddy GD; Kumaraswamy G Photoinduced Electron Transfer (PET) Promoted Cyclisations of 1-[N-alkyl-N-(trimethylsilyl)methyl] amines Tethered to Proximate Olefin: Mechanistic and Synthetic Perspectives. Tetrahedron 1994, 50, 8185.(c)Yoon UC; Mariano PS Mechanistic and Synthetic Aspects of Amine-Enone Single Electron Transfer Photochemistry. Acc. Chem. Res. 1992, 25, 233.(d)Pandey G; Kumaraswamy G; Bhalerao UT Photoinduced, S. E. T. Generation of α-amino radicals: A Practical Method for the Synthesis of Pyrrolidines and Piperidines. Tetrahedron Lett. 1989, 30, 6059.

4. McNally A; Prier CK; MacMillan DWC Discovery of an α-Amino C–H Arylation Reaction Using the Strategy of Accelerated Serendipity. Science 2011, 334, 1114. [PubMed: 22116882]

5. (a)For other methods of α-amino arylation, see: Jiang H-J; Zhong X-M; Yu J; Zhang Y; Zhang X; Wu Y-D; Gong L-Z Assembling a Hybrid Pd Catalyst from a Chiral Anionic CoIII Complex and Ligand for Asymmetric C(sp3)–H Functionalization. Angew. Chem. Int. Ed. 2019, 58, 1803. (b)Greβies S; Klauck FJR; Kim JH; Daniliuc CG; Glorius F Ligand-Enabled Enantioselective Csp^3–H Activation of Tetrahydroquinolines and Saturated Aza-Heterocycles by Rh^1. Angew. Chem. Int. Ed. 2018, 57, 9950.(c)Jain P; Verma P; Xia G; Yu J-Q Enantioselective amine α-functionalization via palladium-catalysed C–H arylation of thioamides. Nat. Chem. 2017, 9, 140. [PubMed: 28282045] (d)Spangler JE; Kobayashi Y; Verma P; Wang D-H; Yu J-Q α-Arylation of Saturated Azacycles and N-Methylamines via Palladium(II)-Catalyzed C(sp3)–H Coupling. J. Am. Chem. Soc. 2015, 137, 11876. [PubMed: 26322957] (e)Peschiulli A; Smout V; Storr TE; Mitchell EA; Eliáš Z; Herrebout W; Berthelot D; Meerpoel L; Maes BUW Ruthenium-Catalyzed α-(Hetero)Arylation of Saturated Cyclic Amines: Reaction Scope and Mechanism. Chem. Eur. J. 2013,19, 10378. [PubMed: 23780756] (f)Campos KR; Klapars A; Waldman JH; Dormer PG; Chen C-Y Enantioselective, Palladium-Catalyzed α-Arylation of N-Boc-pyrrolidine. J. Am. Chem. Soc. 2006, 128, 3538. [PubMed: 16536525] (g)Pastine SJ; Gribkov DV; Sames D sp3 C–H Bond Arylation Directed by Amidine Protecting Group: a-Arylation of Pyrrolidines and Piperidines. J. Am. Chem. Soc. 2006, 128, 14220. [PubMed: 17076471] (h)Li Z; Li C-J CuBr-Catalyzed Direct Indolation of Tetrahydroisoquinolines via Cross-Dehydrogenative Coupling between sp3 C–H and sp2 C–H Bonds. J. Am. Chem. Soc. 2005, 127, 6968. [PubMed: 15884937]

6 (a). Kohls P; Jadhav D; Pandey G; Reiser O Visible Light Photoredox Catalysis: Generation and Addition of N-Aryltetrahydroisoquinoline-Derived α-Amino Radicals to Michael Acceptors. Org. Lett. 2012, 14, 672. [PubMed: 22260623] (b)Miyake Y; Nakajima K; Nishibayashi Y

Visible-Light-Mediated Utilization of α-Aminoalkyl Radicals: Addition to Electron-Deficient Alkenes Using Photoredox Catalysts. J. Am. Chem. Soc. 2012, 134, 3338. [PubMed: 22296639]

7 (a). Gui Y-Y; Sun L; Lu Z-P; Yu D-G Photoredox sheds new light on nickel catalysis: from carbon–carbon to carbon–heteroatom bond formation. Org. Chem. Front. 2016, 3, 522.(b)Zuo Z; Ahneman DT; Chu L; Terrett JA; Doyle AG; MacMillan DWC Merging photoredox with nickel catalysis: Coupling of α-carboxyl sp³-carbons with aryl halides. Science 2014, 345, 437. [PubMed: 24903563]

8 (a). Nakajima K; Miyake Y; Nishibayashi Y Synthetic Utilization of α-Aminoalkyl Radicals and Related Species in Visible Light Photoredox Catalysis. Acc. Chem. Res. 2016, 49, 1946. [PubMed: 27505299] (b)Mitchell EA; Peschiulli A; Lefevre N; Meerpoel L; Maes BUW Direct α-Functionalization of Saturated Cyclic Amines. Chem. Eur. J. 2012, 18, 10092. [PubMed: 22829434] (c)Campos KR Direct sp³ C–H bond activation adjacent to nitrogen in heterocycles. Chem. Soc. Rev. 2007, 36, 1069. [PubMed: 17576475]

9 (a). Meggers E Asymmetric catalysis activated by visible light. Chem. Commun. 2015, 51, 3290. (b)Svoboda J; König B Templated Photochemistry: Toward Catalysts Enhancing the Efficiency and Selectivity of Photoreactions in Homogeneous Solutions. Chem. Rev. 2006, 106, 5413. [PubMed: 17165693]

10. (a)For the photoredox catalyzed enantioselective synthesis of α-branched amines via α-amino radicals, see: Shin NY; Ryss JM; Zhang X; Miller SJ; Knowles RR Light-Driven Deracemization Enabled by Excited-State Electron Transfer. Science 2019, 366, 364. [PubMed: 31624212] (b)Proctor RSJ; Davis HJ; Phipps RJ Catalytic enantioselective Minisci-type addition to heteroarenes. Science 2018, 360, 419. [PubMed: 29622723] (c)Wang C; Qin J; Shen X; Riedel R; Harms K; Meggers E Asymmetric Radical–Radical Cross-Coupling through Visible-Light-Activated Iridium Catalysis. Angew. Chem. Int. Ed. 2016, 55, 685.(d)Zuo Z; Cong H; Li W; Choi J; Fu GC; MacMillan DWC Enantioselective Decarboxylative Arylation of α-Amino Acids via the Merger of Photoredox and Nickel Catalysis. J. Am. Chem. Soc. 2016, 138, 1832. [PubMed: 26849354] (e)Uraguchi D; Kinoshita N; Kizu T; Ooi T Synergistic Catalysis of Ionic Brønsted Acid and Photosensitizer for a Redox Neutral Asymmetric α-Coupling of N-Arylaminomethanes with Aldimines. J. Am. Chem. Soc. 2015, 137, 13768. [PubMed: 26456298] (f)Espelt LR; McPherson IS; Wiensch EM; Yoon TP Enantioselective Conjugate Additions of α-Amino Radicals via Cooperative Photoredox and Lewis Acid Catalysis. J. Am. Chem. Soc. 2015, 137, 2452. [PubMed: 25668687]

11 (a). Leitch JA; Rogova T; Duarte F; Dixon DJ Dearomative Photocatalytic Construction of Bridged 1,3-Diazepanes. Angew. Chem. Int. Ed. 2020, 59, 4121.(b)McManus JB; Onuska NPR; Nicewicz DA Generation and Alkylation of α-Carbamyl Radicals via Organic Photoredox Catalysis. J. Am. Chem. Soc. 2018, 140, 9056. [PubMed: 29986129] (c)Rossolini T; Leitch JA; Grainger R; Dixon DJ Photocatalytic Three-Component Umpolung Synthesis of 1,3-Diamines. Org. Lett. 2018, 20, 6794. [PubMed: 30350662] (d)Aycock RA; Pratt CJ; Jui NT Aminoalkyl Radicals as Powerful Intermediates for the Synthesis of Unnatural Amino Acids and Peptides. ACS Catal. 2018, 8, 9115.(e)Leitch JA; Fuentes de Arriba AL; Tan J; Hoff O; Martínez CM; Dixon DJ Photocatalytic reverse polarity Povarov reaction. Chem. Sci. 2018, 9, 6653. [PubMed: 30310598] (f)Liu J; Xie J; Zhu C Photoredox organocatalytic α-amino C(sp3)–H functionalization for the synthesis of 5-membered heterocyclic γ-amino acid derivatives. Org. Chem. Front. 2017, 4, 2433.(g)Xuan J; Cheng Y; An J; Lu L-Q; Zhang X-X; Xiao W-J Visible light-induced intramolecular cyclization reactions of diamines: a new strategy to construct tetrahydroimidazoles. Chem. Commun. 2011, 47, 8337.

12. Aminomethyl radical additions to the Karady–Beckwith chiral dehydroalanine gave 5-oxazolidinones with high diastereoselectivity; however, for aminoalkyl radical additions providing α-branched amines, little to no diastereoselectivity was observed at the branched site, see: Ref 11d.

13. For photoredox catalyzed generation of an iminium intermediate followed by diastereoselective cyclization to an imidazolidines, see Ref 11g.

14. Escoubet S; Gastaldi S; Vanthuyne N; Gil G; Siri D; Bertrand MP Thiyl Radical Mediated Racemization of Benzylic Amines. Eur. J. Org. Chem. 2006, 3242.

15. See Scheme 3 in Ref 11e.

16. (a)For diastereoselective synthesis by reversible C–C bond formation by photoredox catalysis, see: Stache EE; Rovis T; Doyle AG Dual Nickel- and Photo redox-Catalyzed Enantioselective Desymmetrization of Cyclic meso-Anhydrides. Angew. Chem. Int. Ed. 2017, 56, 3679.(b)Keylor MH; Matsuura BS; Griesser M; Chauvin J-PR; Harding RA; Kirillova MS; Zhu X; Fischer OJ; Pratt DA; Stephenson CRJ Synthesis of resveratrol tetramers via a stereoconvergent radical equilibrium. Science 2016, 354, 1260. [PubMed: 27940867]

17. (a). Duttwyler S; Chen S; Takase MK; Wiberg KB; Bergman RG; Ellman JA Proton Donor Acidity Controls Selectivity in Nonaromatic Nitrogen Heterocycle Synthesis. Science 2013, 339, 678. [PubMed: 23393259] (b)Duttwyler S; Lu C; Rheingold AL; Bergman RG; Ellman JA Highly Diastereoselective Synthesis of Tetrahydropyridines by a C–H Activation–Cyclization–Reduction Cascade. J. Am. Chem. Soc. 2012, 134, 4064. [PubMed: 22356093] (c)Colby DA; Bergman RG; Ellman JA Synthesis of Dihydropyridines and Pyridines from Imines and Alkynes via C-H Activation. J. Am. Chem. Soc. 2008, 130, 3645. [PubMed: 18302381]

18. Wiesenfeldt MP; Nairoukh Z; Dalton T; Glorius F Selective Arene Hydrogenation for Direct Access to Saturated Carbo- and Heterocycles. Angew. Chem. Int. Ed. 2019, 58, 10460.

19. In the absence of catalyst, 10% product is observed (see Table S2). Under our standard reaction conditions, the large majority of visible photons are absorbed by Ir(ppy)3. However, in the absence of Ir(ppy)3, an EDA complex between the DCB and piperidine could result in the small amount of product formed. For a similar result, see: Miao M; Liao L-L; Cao G-M; Zhou W-J; Yu D-G Visible-light-mediated external-reductant-free reductive cross coupling of benzylammonium salts with (hetero)aryl nitriles. Sci. China Chem. 2019, 62, 1519.

20. Shono T; Hamaguchi H; Matsumura Y Electroorganic chemistry. XX. Anodic oxidation of carbamates. J. Am. Chem. Soc. 1975, 97, 4264.

21. The relative stereochemistry for the major and minor diastereomers were determined by NOE correlations (see Supporting Information).

22. Sakamoto M; Cai X; Kim SS; Fujitsuka M; Majima T Intermolecular Electron Transfer from Excited Benzophenone Ketyl Radical. J. Phys. Chem. A 2007, 111, 223. [PubMed: 17214457]

23. Ide T; Barham JP; Fujita M; Kawato Y; Egami H; Hamashima Y Regio- and chemoselective Csp3–H arylation of benzylamines by single electron transfer/hydrogen atom transfer synergistic catalysis. Chem. Sci. 2018, 9, 8453. [PubMed: 30542595]

24. Prier CK; MacMillan DWC Amine α-heteroarylation via photoredox catalysis: a homolytic aromatic substitution pathway. Chem. Sci. 2014, 5, 4173. [PubMed: 26236461]

25. Lowry MS; Goldsmith JI; Slinker JD; Rohl R; Pascal RA; Malliaras GG; Bernhard S Single-Layer Electroluminescent Devices and Photoinduced Hydrogen Production from an Ionic Iridium(III) Complex. Chem. Mater. 2005, 17, 5712.

26. (a). Flamigni L; Barbieri A; Sabatini C; Ventura B; Barigelletti F Photochemistry and Photophysics of Coordination Compounds: Iridium. Top. Curr. Chem. 2007, 281, 143.(b)Dixon IM; Collin J-P; Sauvage J-P; Flamigni L; Encinas S; Barigelletti F A family of luminescent coordination compounds: Iridium(III) polyimine complexes. Chem. Soc. Rev. 2000, 29, 385.

27. Mori Y; Sakaguchi Y; Hayashi H Magnetic Field Effects on Chemical Reactions of Biradical Radical Ion Pairs in Homogeneous Fluid Solvents. J. Phys. Chem. A 2000, 104, 4896.

28. Robinson EA; Schulte-Frohlinde D Pulse Radiolysis of 1,4-Dicyanobenzene in Aqueous Solutions in the Presence and Absence of Thallium(1) Ions. J. Chem. Soc., Faraday Trans. 1 1973, 69, 707.

29. Seo ET; Nelson RF; Fritsch JM; Marcoux LS; Leedy DW; Adams RN Anodic Oxidation Pathways of Aromatic Amines. Electrochemical and Electron Paramagnetic Resonance Studies. J. Am. Chem. Soc. 1966, 88, 3498.

30. Pitre SP; McTiernan CD; Vine W; DiPucchio R; Grenier M; Scaiano JC Visible-Light Actinometry and Intermittent Illumination as Convenient Tools to Study Ru(bpy)3Cl2 Mediated Photoredox Transformations. Sci. Rep. 2015, 5, 16397. [PubMed: 26578341]

31. Cismesia MA; Yoon TP Characterizing chain processes in visible light photoredox catalysis. Chem. Sci. 2015, 6, 5426. [PubMed: 26668708]

32. Leifert D; Studer A The Persistent Radical Effect in Organic Synthesis. Angew. Chem. Int. Ed. 2020, 59, 74.

33. Slinker JD; Gorodetsky AA; Lowry MS; Wang J; Parker S; Rohl R; Bernhard S; Malliaras GG Efficient Yellow Electroluminescence from a Single Layer of a Cyclometalated Iridium Complex. J. Am. Chem. Soc. 2004, 126, 2763. [PubMed: 14995193]

34. Singh K; Staig SJ; Weaver JD Facile Synthesis of Z-Alkenes via Uphill Catalysis. J. Am. Chem. Soc. 2014, 136, 5275. [PubMed: 24678625]

35. Anslyn EV; Dougherty DA Modern Physical Organic Chemistry. University Science Books: Sausalito, CA, 2006; p 1104.

A. Reactions investigated spectroscopically

$$k_{quench} = 2.9 \times 10^9 \quad M^{-1} s^{-1}$$
$$k_{ox,1m} = 2.4 \times 10^7 \quad M^{-1} s^{-1}$$
$$k_{rec} = \geq 2 \times 10^{10} \quad M^{-1} s^{-1}$$

B. Piperidine oxidation observed as Ir(ppy)$_3^+$ reduction at 390 nm

- 50 mM **1m**
- 25 mM **1m**
- 10 mM **1m**
- 5 mM **1m**
- 0 mM **1m**

C. Charge recombination observed as DCB$^{\bullet-}$ oxidation at 346 nm

- 50 mM **1m**
- 1 mM **1m**

D. Proposed closed-loop mechanism for C-H arylation

Figure 1.

Mechanistic studies (A) Reactions studied by TA and luminescence spectroscopies. (B) TA data collected at 390 nm with 10 mM DCB, 40 μM Ir(ppy)$_3$, and increasing concentrations of **1m**. The laser flash leads to rapid oxidation of the Ir(ppy)$_3^{3+}$, yielding a large negative absorbance change because the Ir(ppy)$_3^+$ species has a smaller ε_{390} than Ir(ppy)$_3$ (Figure S3). **1m** oxidation by Ir(ppy)$_3^+$ is observed as a return in the absorbance at 390 nm as Ir(ppy)$_3^+$ is reduced to Ir(ppy)$_3$. Residual DCB$^{\bullet-}$ absorbance was observed at higher concentrations of **1m**. (C) TA spectroscopy at 346 nm to monitor DCB$^{\bullet-}$ reactivity. (D) Proposed photoredox cycle.
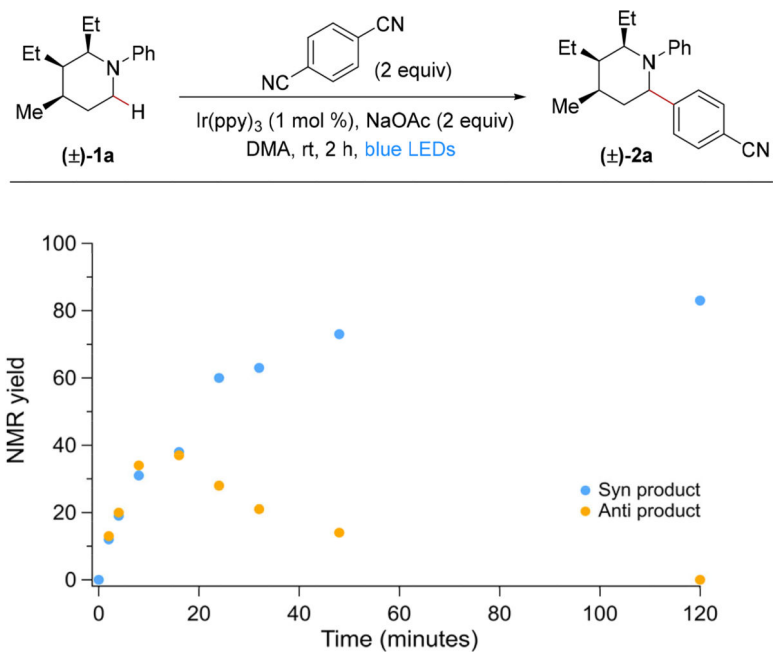
Figure 2.
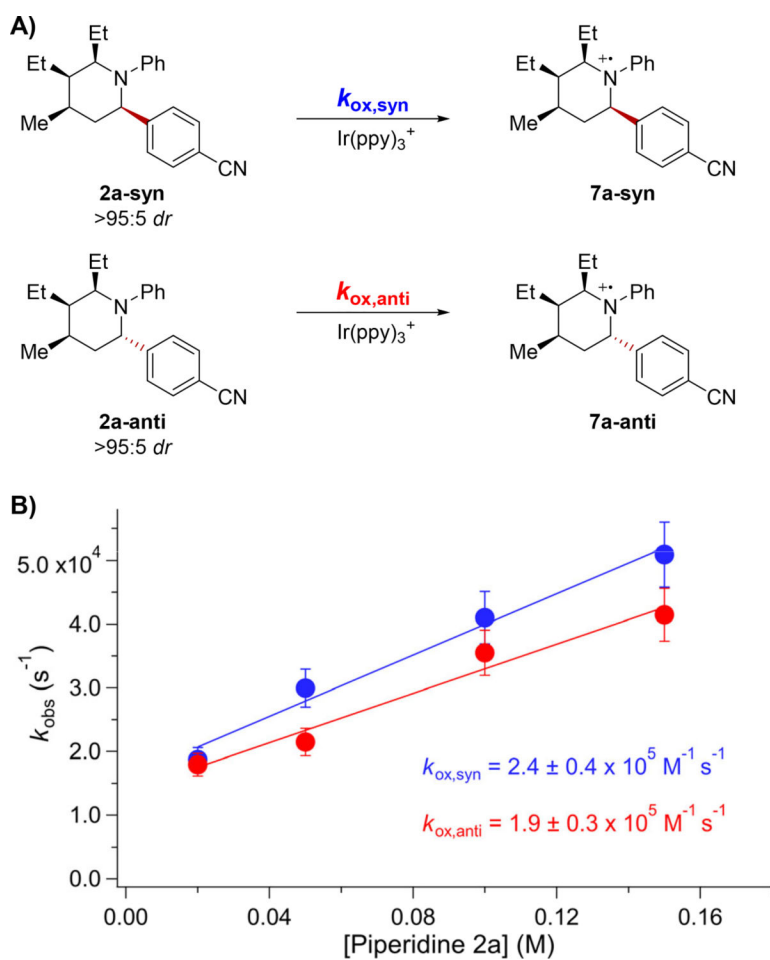Time course studies of the C–H arylation of **1a** and follow-up epimerization of **2a**.

Figure 3.
A) Oxidation reactions investigated for stereoisomerically pure **2a** diastereomers. B) Plot of observed oxidation rate constant versus **2a** concentration, where the slope is k_{ox} for the respective diastereomers. $k_{ox,anti}$ and $k_{ox,syn}$ are within error of each other.
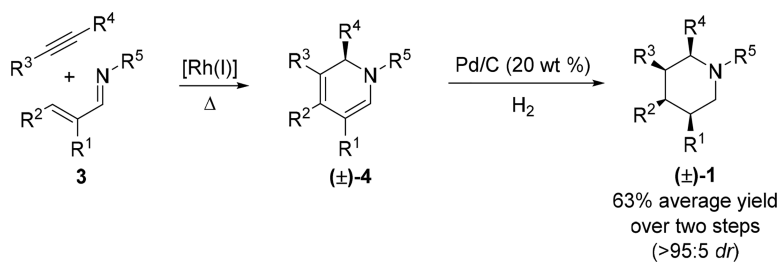
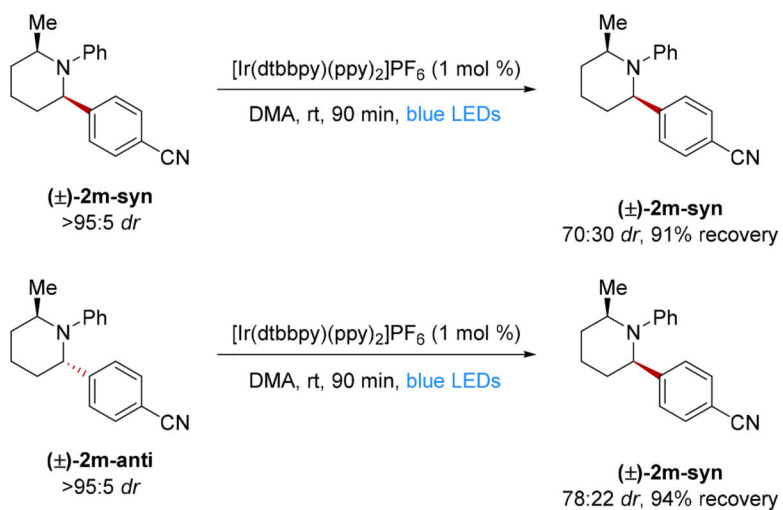**A.** Previously reported α-amino C-H arylation (MacMillan, 2011)
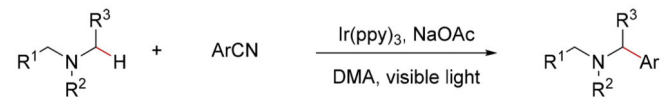
B. *This work:* Diastereoselective C-H arylation of highly substituted piperidines
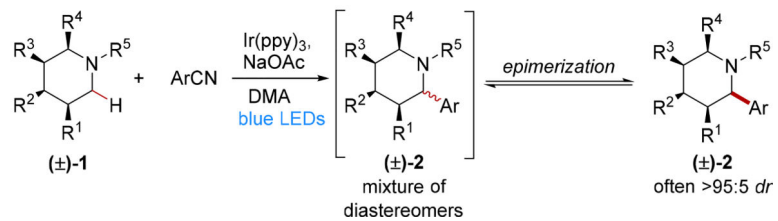
Scheme 1.
Photoredox catalyzed α-amino C–H arylation

Scheme 2.
Highly diastereoselective two-step synthesis of densely substituted piperidines

Scheme 3.
Equilibration of 2m-syn and 2m-anti diastereomers[a]

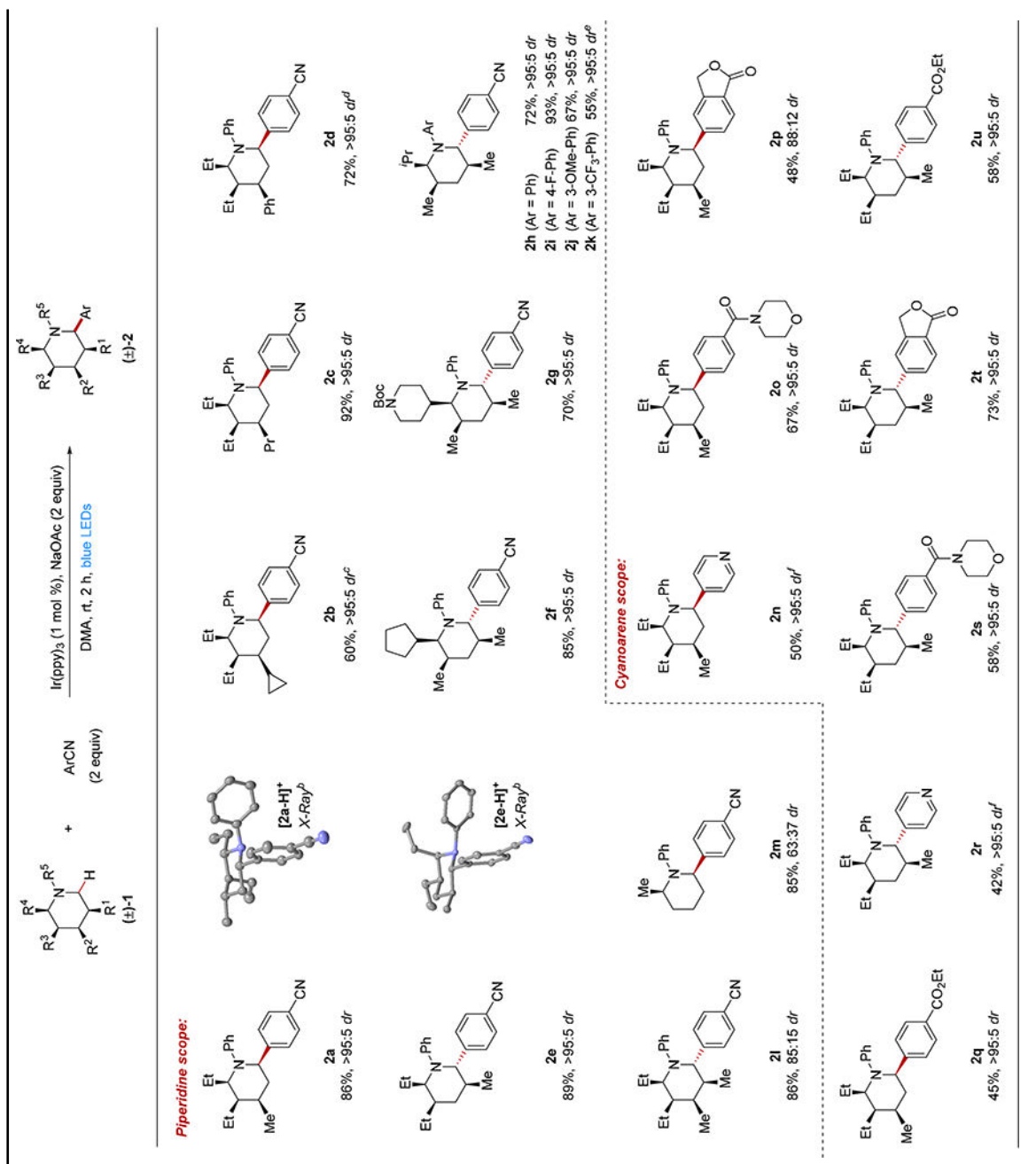[a]Yields determined by ^{1}H NMR spectroscopy with 2,6-dimethoxytoluene as the external standard.

Table 1.

Substrate scope[a]

Reaction scheme:

(±)-1 + ArCN (2 equiv) → Ir(ppy)₃ (1 mol %), NaOAc (2 equiv), DMA, rt, 2 h, blue LEDs → (±)-2

Piperidine scope:

2a — 86%, >95:5 dr
2b — 60%, >95:5 dr[c]
2c — 92%, >95:5 dr
2d — 72%, >95:5 dr[d]

2e — 89%, >95:5 dr
2f — 85%, >95:5 dr
2g — 70%, >95:5 dr

2h (Ar = Ph) — 72%, >95:5 dr
2i (Ar = 4-F-Ph) — 93%, >95:5 dr
2j (Ar = 3-OMe-Ph) — 67%, >95:5 dr
2k (Ar = 3-CF₃-Ph) — 55%, >95:5 dr[e]

2l — 86%, 85:15 dr
2m — 85%, 63:37 dr
2n — 50%, >95:5 dr[f]
2o — 67%, >95:5 dr
2p — 48%, 88:12 dr

2q — 45%, >95:5 dr
2r — 42%, >95:5 dr[f]
2s — 58%, >95:5 dr
2t — 73%, >95:5 dr
2u — 58%, >95:5 dr

Cyanoarene scope:

[2a-H]⁺ X-Ray[b]

[2e-H]⁺ X-Ray[b]

Author Manuscript

Author Manuscript

Author Manuscript

Author Manuscript

[a] Isolated yields on 0.2 mmol scale; *dr* was determined by ^{1}H NMR analysis of the purified product and was within a single percentage point relative to the crude *dr*.

[b] X-ray structure shown with anisotropic displacement ellipsoids at the 50% probability level. The picryl sulfonate counterion and hydrogen atoms are omitted for clarity.
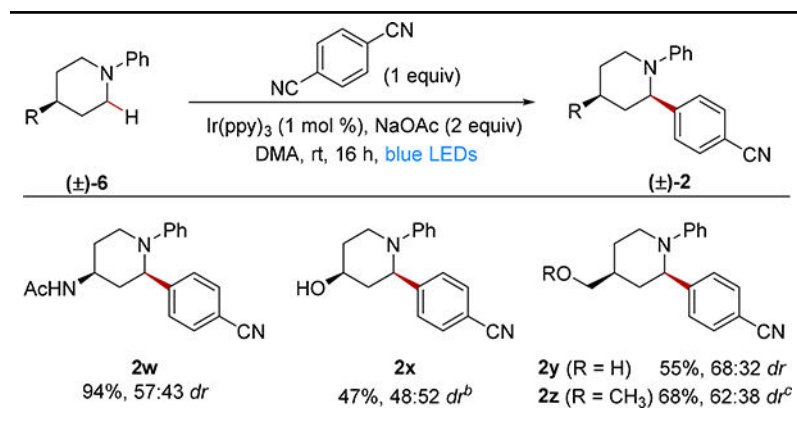
[c] 87:13 *dr* prior to isolation determined by crude ^{1}H NMR analysis.

[d] 16 h reaction time.

[e] 2 mol % Ir(ppy)$_3$, 72 h reaction time.

[f] [Ir(dtbbpy)(ppy)2]PF$_6$ instead of Ir(ppy)3.

Table 2.

Examining scope with 4-substituted piperidines[a]

2w
94%, 57:43 *dr*

2x
47%, 48:52 *dr*[b]

2y (R = H)   55%, 68:32 *dr*
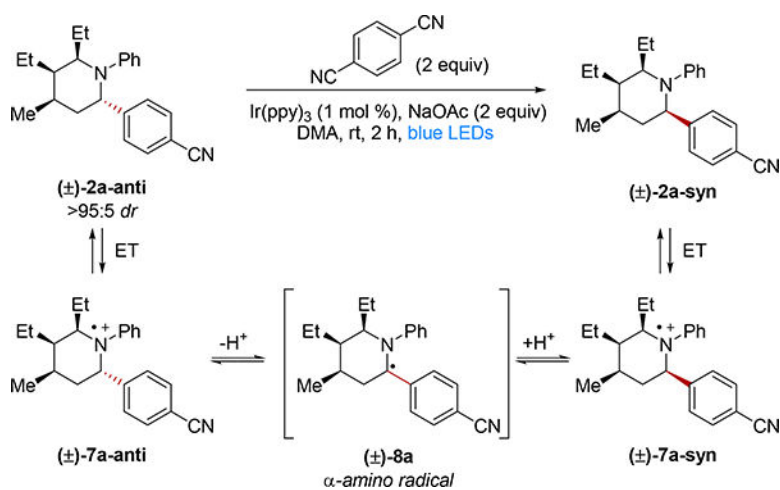**2z** (R = CH$_3$) 68%, 62:38 *dr*[c]

[a]Isolated yields on 0.2 mmol scale; *dr* was determined by ^{1}H NMR analysis of the purified product and was within a single percentage point relative to the crude *dr*.

[b]1:1 *dr* prior to isolation determined by crude ^{1}H NMR analysis.

[c]59:41 *dr* prior to isolation determined by crude ^{1}H NMR analysis.

Table 3.

Evaluating epimerization conditions

entry[a]	conditions	% recovered 2a-anti	% yield 2a-syn
1	Standard conditions	<5	85
2	No NaOAc	<5	74
3	No DCB	67	21
4	No NaOAc, no DCB	62	15
5[b]	No NaOAc, no DCB, [Ir(dtbbpy)(ppy)$_2$]PF$_6$	<5	72

[a]Yields determined by ^{1}H NMR spectroscopy with 2,6-dimethoxytoluene as the external standard.

[b]16 h reaction time.

Table 4.

Calculated relative energies

entry[a]	substrate	exptl. *dr* syn/anti	exptl. G_{anti}- G_{syn}	calculated G_{anti}- G_{syn}
1	**2m**	63:37	0.3 – 0.7	0.6
2	**2a**	>95:<5	>1.8	1.3
3	**2e**	<5:>95	<−1.8	−4.3

[a]Level of theory: ωB97X-D/6-311++G(d,p), CPCM (DMA) // ωB97X-D/6-31G(d), CPCM (DMA).

Exptl. = experimental.